

EPA-600/R-97-079
August 1997

**AN EXPERIMENTAL EVALUATION OF A NOVEL FULL-SCALE
EVAPORATIVELY COOLED CONDENSER**

by

Yunho Hwang
Reinhard Radermacher


Center for Environmental Energy Engineering
University of Maryland
College Park, Maryland 20742-3035

EPA Cooperative Agreement
CR 824187

EPA Project Officer:
Robert V. Hendriks

Air Pollution Prevention and Control Division
National Risk Management Research Laboratory
Research Triangle Park, North Carolina 27711

Prepared for the
U.S. Environmental Protection Agency
Office of Research and Development
Washington, D.C. 20460

TECHNICAL REPORT DATA <i>(Please read Instructions on the reverse before complet</i>		
1. REPORT NO. EPA-600/R-97-079	2.	3.  PB98-100506
4. TITLE AND SUBTITLE An Experimental Evaluation of a Novel Full-scale Evaporatively Cooled Condenser	5. REPORT DATE August 1997	
	6. PERFORMING ORGANIZATION CODE	
7. AUTHOR(S) Yunho Hwang and Reinhard Radermacher	8. PERFORMING ORGANIZATION REPORT NO.	
9. PERFORMING ORGANIZATION NAME AND ADDRESS The University of Maryland Center for Environmental Energy Engineering College Park, Maryland 20742-3035	10. PROGRAM ELEMENT NO.	
	11. CONTRACT/GRANT NO. CR 824187	
12. SPONSORING AGENCY NAME AND ADDRESS EPA, Office of Research and Development Air Pollution Prevention and Control Division Research Triangle Park, NC 27711	13. TYPE OF REPORT AND PERIOD COVERED Final; 1-12/96	
	14. SPONSORING AGENCY CODE EPA/600/13	
15. SUPPLEMENTARY NOTES APPCD project officer is Robert V. Hendriks, Mail Drop 63, 919/ 541-3928.		
16. ABSTRACT The report compares the performance of a novel evaporatively cooled condenser with that of a conventional air-cooled condenser for a split-system heat pump. The system was tested in an environmentally controlled test chamber that is able to simulate test conditions as specified by ASHRAE Standard 116-1983. Soft optimizations were conducted to determine optimum charge and short tube restrictor size. Design parameters of the evaporatively cooled condenser were also optimized experimentally to maximize performance. Using these optimum parameters, steady state and cyclic performance tests were conducted. The experimental results show that the evaporatively cooled condenser has a higher capacity by 1.9 to 8.1%, a compatible coefficient of performance (COP) ranging from 98.0 to 105.6%, and a higher seasonal energy efficiency ratio (SEER) by 11.5% than those of the baseline. Subtracting out the estimated appropriate parasitic power necessitated by the test setup, savings were determined to be 1.8 to 8.1% in capacity, 13.5 to 21.6% in COP, and 14.5% in SEER over the baseline.		
17. KEY WORDS AND DOCUMENT ANALYSIS		
a. DESCRIPTORS	b. IDENTIFIERS/OPEN ENDED TERMS	c. COSATI Field/Group
Pollution Heat Pumps Condensers Test Chambers	Pollution Control Stationary Sources	13B 13A 13I,07A 14B
18. DISTRIBUTION STATEMENT Release to Public	19. SECURITY CLASS (This Report) Unclassified	21. NO. OF PAGES 40
	20. SECURITY CLASS (This page) Unclassified	22. PRICE

NOTICE

This document has been reviewed in accordance with U.S. Environmental Protection Agency policy and approved for publication. Mention of trade names or commercial products does not constitute endorsement or recommendation for use.

FOREWORD

The U.S. Environmental Protection Agency is charged by Congress with protecting the Nation's land, air, and water resources. Under a mandate of national environmental laws, the Agency strives to formulate and implement actions leading to a compatible balance between human activities and the ability of natural systems to support and nurture life. To meet this mandate, EPA's research program is providing data and technical support for solving environmental problems today and building a science knowledge base necessary to manage our ecological resources wisely, understand how pollutants affect our health, and prevent or reduce environmental risks in the future.

The National Risk Management Research Laboratory is the Agency's center for investigation of technological and management approaches for reducing risks from threats to human health and the environment. The focus of the Laboratory's research program is on methods for the prevention and control of pollution to air, land, water, and subsurface resources; protection of water quality in public water systems; remediation of contaminated sites and groundwater; and prevention and control of indoor air pollution. The goal of this research effort is to catalyze development and implementation of innovative, cost-effective environmental technologies; develop scientific and engineering information needed by EPA to support regulatory and policy decisions; and provide technical support and information transfer to ensure effective implementation of environmental regulations and strategies.

This publication has been produced as part of the Laboratory's strategic long-term research plan. It is published and made available by EPA's Office of Research and Development to assist the user community and to link researchers with their clients.

E. Timothy Oppelt, Director
National Risk Management Research Laboratory

ABSTRACT

In this report, the performance of a novel evaporatively cooled condenser is compared with that of a conventional air-cooled condenser for a split heat pump system. The system was tested in an environmentally controlled test chamber that is able to simulate test conditions as specified by ASHRAE Standard 116-1983. Using refrigerant HCFC-22, soft optimizations were conducted to determine optimum charge and short tube restrictor size. Design parameters of the evaporatively cooled condenser were also optimized experimentally to maximize the performance. Using these optimum parameters, steady state and cyclic performance tests were conducted.

The experimental results show that the evaporative condenser has a higher capacity by 1.8 to 8.1 %, a compatible COP ranging from 98.0 to 105.6 %, and a higher SEER by 11.5 % than those of the baseline. Subtracting out the estimated appropriate parasitic power necessitated by the test setup, savings are 1.8 to 8.1% in the capacity, 13.5 to 21.6 % in the COP, and 14.5 % in the SEER.

TABLE OF CONTENTS

<u>Section</u>	<u>Page</u>
ABSTRACT	iv
LIST OF TABLES	vii
LIST OF FIGURES	viii
NOMENCLATURE	ix
1.0 INTRODUCTION	1
2.0 TEST FACILITY AND TEST UNIT	2
2.1 Test Facility	2
2.2 Test Unit	3
3.0 INSTRUMENTATION AND TEST PROCEDURE	6
3.1 Test Condition	6
3.2 Instrumentation	6
3.3 Data Acquisition System	8
3.4 Performance Calculation	8
3.5 Test Procedures	8
4.0 TEST RESULTS AND DISCUSSION	9
4.1 Charge Optimization Test Results at ASHRAE Test A	9
4.2 System Performance Test Results with Charge Optimized at ASHRAE Test A ...	11
4.3 Charge Optimization Test Results at ASHRAE Test B	11
4.4 Airflow Optimization Test Results at ASHRAE Test B	13
4.5 Wheel Rotation Speed Optimization Test Results at ASHRAE Test B	13
4.6 Steady State Performance Test Results	14
4.7 Cyclic Performance Test Results	15
4.8 Fan and Wheel Motor Power Compensation Results	16
4.9 Thermal Storage Effect Test Results	17
5.0 CONCLUSIONS	19
ACKNOWLEDGMENT	19
REFERENCES	19

TABLE OF CONTENTS

<u>Section</u>	<u>Page</u>
Appendix A-1 Evaporative Condenser Performance Evaluation	A-1
Appendix A-2 Instruments	A-5
Appendix A-3 Uncertainty Analysis	A-7
Appendix A-4 Quality Assurance	A-9
Appendix A-5 References	A-11

LIST OF TABLES

<u>Number</u>	<u>Page</u>
1. ASHRAE 116-1983 Test Conditions (Cooling Only)	6
2. Optimum Charge Test Results for Each ST at ASHRAE Test A Condition	10
3. Steady State ASHRAE Test Results	10
4. Cyclic ASHRAE Test Results	11
5. Optimum Charge Test Results at ASHRAE Test B Condition (ST: 0.067")	13
6. Airflow Optimization Test Results (Charge: 9.0 lb, ST: 0.067")	14
7. Wheel Rotation Speed Optimization Test Results (Charge: 9.0 lb, ST: 0.067")	14
8. Steady State ASHRAE Test Results	15
9. Seasonal Performance Test Results	16
10. Fan and Wheel Motor Power Compensation	16
11. Compensated Steady State ASHRAE Test Results	17
12. Compensated Seasonal Performance Test Results	17
A-1. Estimated Bias Errors of Characteristic Parameters	A-7
A-2. Estimated Random Errors of Characteristic Parameters	A-8
A-3. Estimated Total Uncertainty of Characteristic Parameters	A-8

LIST OF FIGURES

<u>Number</u>	<u>Page</u>
1. Indoor Loop	4
2. Heat Pump System Layout	4
3. Evaporative Condenser	5
4. Charge Optimization with Various Short Tube Sizes	12
5. Charge Optimization at ASHRAE Test B	12
6. Cyclic Test (ASHRAE Test D): Compressor, Outdoor Fan & Wheel All Cycle	18
7. Cyclic Test (ASHRAE Test D): Outdoor Fan & Wheel Running Continuously	18

NOMENCLATURE

ASHRAE	American Society for Heating, Refrigerating and Air-Conditioning Engineers
ARI	American Refrigeration Institute
C_D	Cyclic Degradation Coefficient
CLF	Cooling Load Factor
COP	Coefficient of Performance
HCFCs	Hydrochlorofluorocarbons
R-22	Refrigerant 22, Trifluoromethane
P_{cond}	Condensing Pressure
P_{evap}	Evaporating Pressure
SEER	Seasonal Energy Efficiency Ratio
ST	Short Tube Restrictor

1.0 INTRODUCTION

There are three main types of condensers used in heat pump systems: air-cooled, water-cooled, and evaporatively cooled. Condensers used in conventional split heat pump systems are mainly air-cooled; they depend on the heat transfer between the coils and the airflow. In this regard, air-cooled condensers need a high airflow rate for higher performance. Used less commonly, water-cooled condensers depend on the heat transfer between the coils and a water flow. Water-cooled condensers have a higher heat transfer coefficient than air-cooled condensers. However, they require a water pump to circulate the water and chemical treatment of the water to reduce fouling of the coils. Evaporatively cooled condensers have been used extensively to enhance heat transfer and improve performance of cooling systems. A popular design for an evaporatively cooled condenser (hereafter called as “evaporative condenser”) is to spray water onto the condenser tubes as air is simultaneously blown over them. The water that is not evaporated then drains to the bottom of the condenser unit and is pumped up to the sprayers using a water pump. Cooling is accomplished by the evaporation of the water into the air-stream. Thus, the water pumping and chemical treatment requirement of the water-cooled condensers are reduced. The high airflow rate required from the air-cooled condensers is also significantly reduced. [1]

On the other hand, there are some disadvantages of the evaporative condenser. First, it is more appropriate for central cooling systems than for heat pumps because of freezing of the water in the outside heat exchanger during cold weather home heating. For cooling only, controllers can be provided so that the water is drained automatically when the system is shut down for the season. Second, the water pool may pose a health hazard as biological growth, such as legionella, may develop. [2] Some minimal amount of water treatment is needed to prevent algae growth. This has always been one of the drawbacks of wet systems for homeowners as they do not want to maintain such a system or will forget to maintain it. For this type of evaporative condenser, however, there is such a small water flow that a package treatment system is available that will not require homeowner maintenance for the life of the unit.

In the design studied in this report, the condenser tubes are immersed in a water bath, as in a water-cooled condenser. Wheel disks, which are partially submerged in the bath, are rotated by a direct-drive motor while air is blown across them. The disks carry a thin water film from the bath to the air stream and this water film is evaporated into the air stream. The condenser tubes reject heat to the water bath and the evaporation of the water film rejects heat to the air stream. System reliability is increased in this design because it eliminates the need for a water pump. Also, the airflow rate required is less than that of an air-cooled condenser.

The major advantage of the evaporative condenser is that the condensing temperature is lower than that of an air-cooled condenser. The condensing temperature of this design is limited by the wet bulb temperature of the air rather than the dry bulb temperature. Since the wet bulb temperature is usually 14 to 25 F° (8 to 14 C°) lower than the dry bulb temperature, the condensing temperature is lowered. [2] The lower condensing temperature reduces the pressure across the compressor, reducing the work done by the compressor and thereby increasing the COP. Previous tests have shown that the compressor power consumption is reduced by 11.4% and the COP is increased by 20% as compared to conventional condensers. [2]

In summary, the advantages of the evaporative condenser can be listed as following.

- Low cost / Light weight (wheel disks are made of plastic.)
- Minimal air pressure drop / Low fan motor power
- Great potential for performance improvement
- Low condensing and compressor discharge temperature / Higher system reliability

2.0 TEST FACILITY AND TEST UNIT

Steady state and cyclic performance testing of the evaporative condenser is performed inside an environmentally controlled chamber capable of simulating cooling and heating conditions as specified by ASHRAE Standard 116-1983. [3] A two-way duct, capable of replacing the humid air exiting the condenser with fresh outside air, keeps the humidity constant inside the chamber. The evaporative condenser is retrofitted onto an existing 2.5 ton split heat pump system. For the purposes of this test, the heat pump only operates in the cooling mode using a short tube restrictor (ST) as the expansion device. The refrigerant used is HCFC-22 (R-22).

2.1 Test Facility

The heat pump system with the evaporative condenser prototype was tested in CEEE's existing environmental simulation facilities. The test facility is composed of two sections, which separately simulate indoor and outdoor conditions. A closed air loop holds the heat pump's indoor unit and maintains indoor conditions, while a controlled-environment chamber holds the compressor and condenser unit and maintains simulated outdoor conditions. The test facility was constructed to be in compliance with ASHRAE Standard 116-1983. [3]

Indoor Loop

As shown in Figure 1, the indoor loop is a vertical rectangle of sealed and insulated duct, with two horizontal and two vertical legs. The heat pump's indoor unit (the evaporator and fan) is mounted in one of the vertical sections, with air flowing downward through the coils. The upper duct houses the loop's climate-control equipment. This includes electrical resistance heaters, a cooling coil, a separate condensing coil to remove moisture from the loop air, and a steam generator to inject moisture into the loop. All these devices are managed by a Proportion Integration Differentiation (PID) controller, which reacts to the changing loads from the evaporator to keep the loop air at the desired temperature and relative humidity. Loop air is circulated by a large centrifugal blower connected to a variable-frequency AC inverter. The inverter's output frequency can be changed to adjust the blower speed and thus the air flow rate.

Outdoor Chamber

The Outdoor Chamber is an insulated room approximately 5m x 5.5m. Its array of control equipment is similar to that of the indoor loop, except that the dehumidification is handled by a desiccant-wheel dryer using silica gel. The PID controller maintains the preset outdoor conditions. Although the chamber was designed to operate as a closed system, its equipment was not sized to

remove as much moisture as the evaporative condenser unit produces. Therefore, an exhaust duct was installed to channel humid air from the condenser outlet out of the building. Leaving the chamber door slightly ajar allowed make up air to enter, and the moisture load was reduced to manageable levels. The PID controller's input comes from a combined electronic temperature and relative humidity sensor which is placed at the entrance to the evaporative condenser's inlet air duct.

2.2 Test Unit

The test unit was a Trane heat pump (Weathertron XE 1100) whose outdoor unit (air-cooled condenser and fan) was replaced with the evaporative condenser prototype. The original system's compressor was retained. The performance data cited in this report for the "evaporative condenser" system are for this combination. Tests of the unaltered Trane heat pump system, as installed in CEEE's test facility, supplied the baseline performance data to which the experimental system is compared. The layout of heat pump system is shown in Figure 2.

- *Heat Pump System:* The major components of this system are the Trane evaporator and indoor blower which are installed in the indoor loop, the Trane system compressor in the outdoor chamber; the evaporative condenser itself, also in the outdoor chamber, and the connecting refrigerant tubing.
- *Indoor Unit:* The evaporator and indoor blower, as mentioned, are from the original Trane heat pump system. The test system uses a short tube restrictor to expand the refrigerant as it enters the evaporator.
- *Compressor:* The Trane system compressor was removed from the Trane outdoor air-cooled condenser unit and installed in a more accessible location near the evaporative condenser in the outdoor chamber.
- *Connecting Tubes:* High-pressure-side connecting tubes are 3/8" copper, and low-pressure-side tubing is 5/8" copper. Joints are either soldered or use flare fittings or Swage-Lock compression fittings.
- *Evaporative Condenser:* The evaporative condenser is located in the outdoor chamber. Its three main components are the condenser tank, the inlet duct and exhaust duct, and the wheel disks and motor. The condenser tank is an acrylic box, 0.94m wide x 0.66m long x 0.66m high. The inlet and exhaust ducts connect to openings in this box, size 0.33m x .91m. A valved water-supply line allows the water level in the tank to be maintained at a depth of 0.25m during operation, which ensures that the condenser tubes are fully immersed. The condenser is built of 3/8" copper tubes arranged in a stack of four horizontal arrays; each array is horizontally offset from the arrays above and below, as shown in Figure 3. This leaves narrow, regularly-spaced gaps between adjacent tubes. A transverse-mounted axle holds 35 double-faced corrugated plastic disks (0.6m diameter), and is rotated via a belt connected to a variable-speed electric motor mounted next to the tank. The disks are partially submerged in the water bath, and pass between the banks of condenser tubes. A centrifugal blower (with a 0.25m diameter wheel) pulls air into the inlet duct, where a honeycomb baffle and flow-straightening vanes ensure relatively uniform flow distribution. From the inlet duct, air flows into the condenser box, between the rotating disks, and out of

Figure 1 Indoor Loop

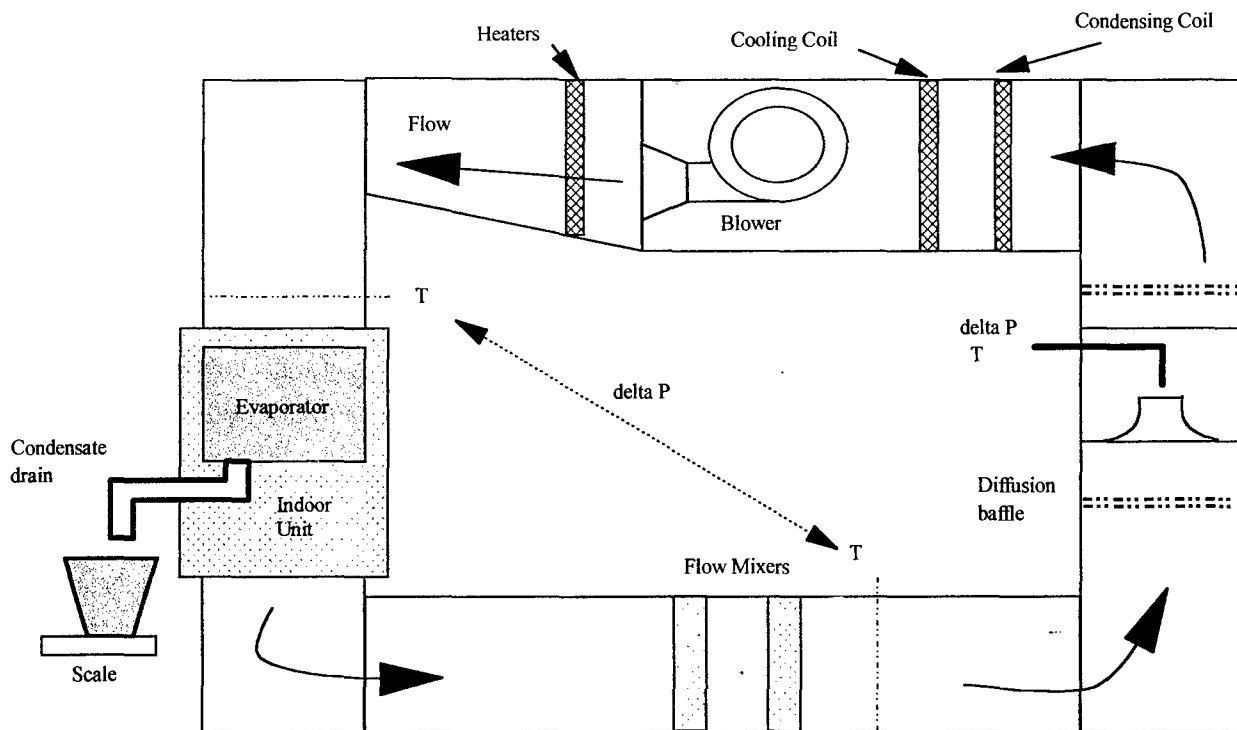


Figure 2 Heat Pump System Layout

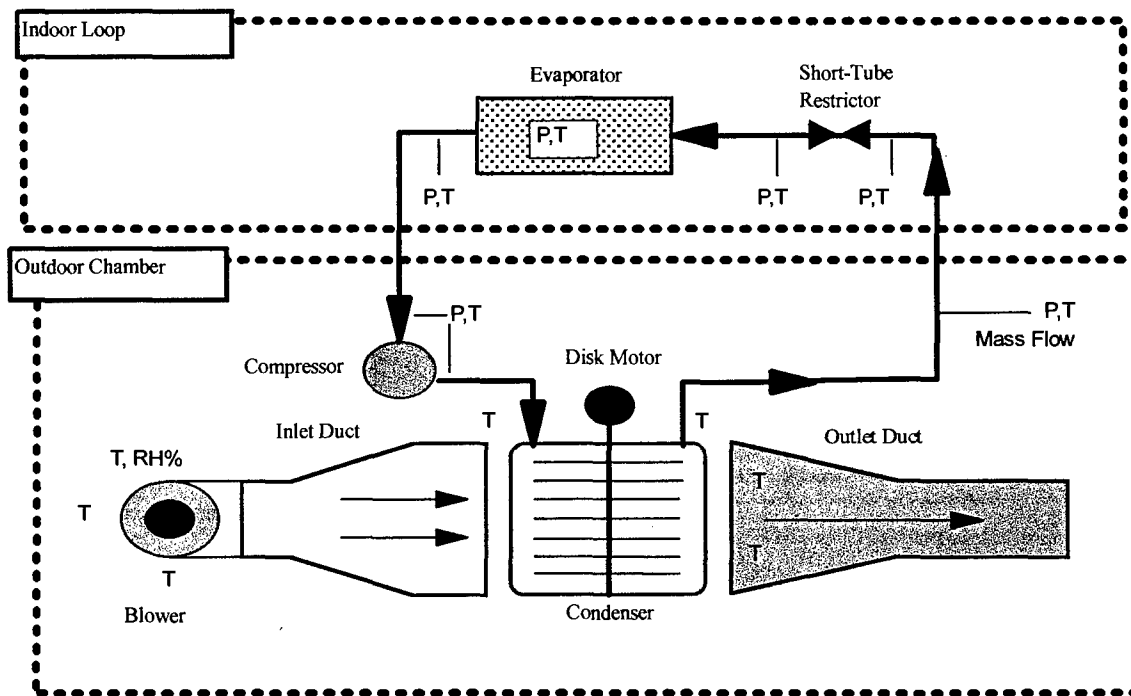
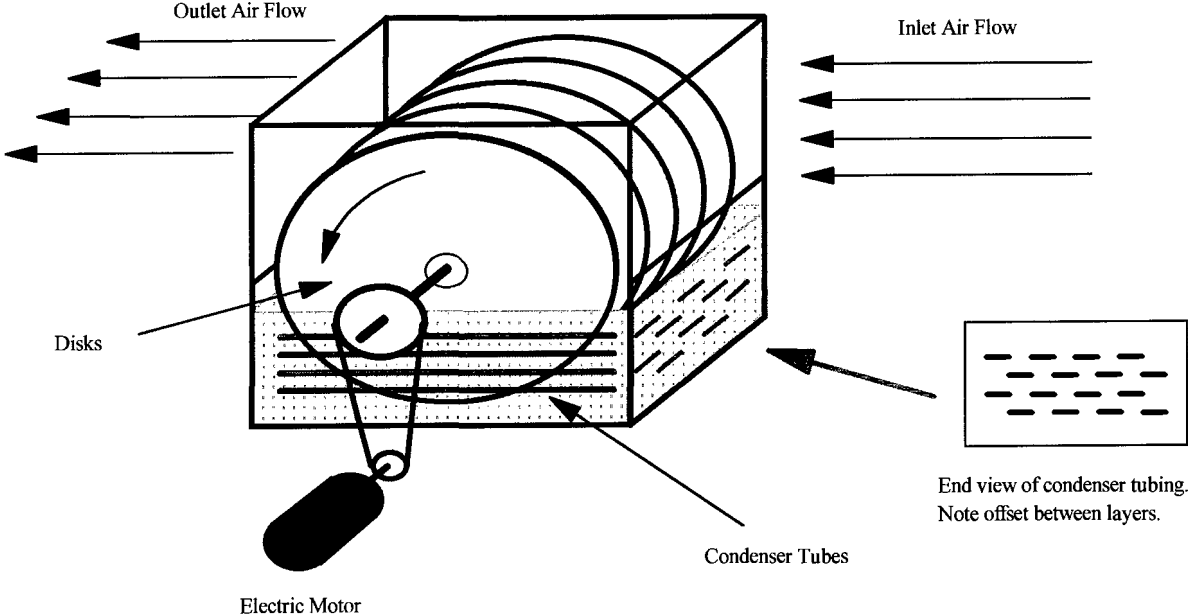


Figure 3 Evaporative Condenser



the building via the exhaust duct. This is a “parallel-flow” arrangement, with air flowing parallel to the plane of the disks along their entire exposed surface area.

- *General Description of Evaporative Condenser Heat Rejection Mechanism:* As the disks rotate, their wetted surfaces pull a film of water out of the bath into the airstream. The passing air evaporates some of the water film, cooling the water which remains on the disks. This cooled water is returned to the bath as the disk rotates, cooling the bath and thus the condenser tubes. [2]

3.0 INSTRUMENTATION AND TEST PROCEDURE

3.1 Test Condition

The experiments to measure the capacity and COP of the system were performed based on ASHRAE Standard 116-1983 [3], and ARI Standard 210/240. [4] Table 1 lists the ASHRAE Test Conditions for the cooling tests. The cooling capacity was calculated on the air-side and the refrigerant-side of the evaporator (indoor coil).

Table 1 ASHRAE 116-1983 Test Conditions (Cooling Only) (Unit: [°F(°C)])

TEST	INDOOR		OUTDOOR		OPERATION
	D.B.	W.B.	D.B.	W.B.	
A	80 (26.7)	67 (19.4)	95 (35.0)	75 (23.9)	Steady State Cooling
B	80 (26.7)	67 (19.4)	82 (27.8)	65 (18.3)	Steady State Cooling
C	80 (26.7)	<57 (13.9)	82 (27.8)	65 (18.3)	S.S. Cooling, Dry Coil
D	80 (26.7)	<57 (13.9)	82 (27.8)	65 (18.3)	Cyclic Cooling, Dry Coil

[Note] D.B.: Dry-bulb Temperature
W.B.: Wet-bulb Temperature

3.2 Instrumentation

Indoor Air-Side Instrumentation

The Indoor Loop is equipped to measure the evaporator’s performance by monitoring loop air conditions.

- *Temperature Change:* two 9-element thermocouple grids measure air temperature change due to the heat absorbed by an evaporator. One is placed just upstream, after the main blower. The downstream grid is placed after two flow mixers, which ensure uniform flow temperature. Each grid’s 9 readings are averaged for one overall flow temperature at that point.
- *Evaporator Pressure Drop:* This is recorded by pressure taps just before and after the evaporator, which are connected to an electronic differential pressure transducer (Setra Model 264).

- *Air Flow Rate:* A calibrated nozzle is mounted in the second vertical duct to create a high-velocity flow, which is accurately measured by a Pitot tube. The pressure drop across the nozzle is also recorded by pressure taps and another Setra differential pressure transducer. These readings allow the volume and mass flow of air to be calculated using relations described in ANSI Standard 210-1985. [5]
- *Condensate Mass:* Water condensed from the loop air by the evaporator is caught in a drip tray, and drains through PVC tubes to a collection bucket. This bucket is weighed on an electronic scale before and after a test to determine the mass of condensate produced. A trap in the condensate drain tube prevents loop air from escaping.
- *Relative Humidity:* A combined electronic temperature and relative-humidity sensor are connected to the loop's PID controller. This sensor is placed just upstream of the evaporator.

Evaporative Condenser Instrumentation

The following quantities are measured to allow analysis of the condenser's performance:

- *Inlet Relative Humidity:* The PID controller's electronic sensor is placed at the entrance of the inlet duct; its readout may be taken from the environmental chamber's control panel. In addition, a General Eastern Hygro-M2 Humidity Monitor is set up to sample air at the same point. The two devices' outputs are compared as a check.
- *Inlet Temperature:* A "rake" of 9 thermocouples is arranged around the entrance to the inlet duct. The readings are averaged to yield one inlet air temperature.
- *Outlet Temperature:* Six thermocouples are hung in the airstream at the condenser exit. Their average reading is taken as the outlet air temperature.
- *Inlet Duct Flow Velocity:* A Pitot tube connected to a differential pressure transducer is introduced into the inlet duct near the evaporator box entrance and scanned across cross section. Use of the Pitot equation yields the flow velocity, from which volume and mass flow of air can be calculated.
- *Water Bath Temperature:* Five thermocouples are immersed in the condenser water bath; three are near the wheel disk's exit side of the tank and two near the entrance side. Their averaged readings provide the overall bath temperature. Aside from measuring thermal storage effects of the bath, the distributed thermocouples' individual readings can be used to verify uniform temperature distribution in the bath.

Refrigerant-Side Instrumentation

- *Refrigerant Pressure:* Electronic absolute pressure transducers (Setra Model 280E, 0-500 psia) are installed at a number of points in the refrigerant loop:
 - Before and after the short tube restrictor at the evaporator entrance
 - At the evaporator exit
 - On the compressor suction and discharge lines
 - After the condenser exit, at the mass-flow meter
- *Refrigerant mass flow rate:* A refrigerant mass-flow rate is measured by a Micro motion

mass-flow meter downstream of the condenser exit.

- *Refrigerant temperature:* Refrigerant temperature measurements are taken by Type T (copper-constantan) thermocouples either soldered or fixed with aluminum HVAC tape to the tube. Measurements are taken:
 - Before and after the short tube restrictor at the evaporator entrance
 - At each pass along the length of the evaporator tubing
 - At the evaporator exit
 - Compressor suction and discharge lines; also on the compressor casing itself
 - At the condenser entrance, on each of the four arrays of condenser tubing
 - At the condenser exit, on each tubing array
 - At the refrigerant mass-flow meter inlet

3.3 Data Acquisition System

The thermocouples, pressure transducers and mass-flow meter are connected to three Hewlett Packard 7500 Series B data acquisition mainframes. These perform some data preprocessing (converting thermocouple voltages to degrees Celsius, for example) and pass the data to a custom-designed monitoring and control program running in the HP Visual Basic environment on a personal computer. This program converts the rest of the sensor data to engineering units and saves all data to ASCII-text data files. The program also displays selected channels' data as text and graphically; the display is updated with each scan.

This program also controls the test system via power relays. For cyclic tests, the program can turn on and off the indoor blower, the compressor, the outdoor blower, and the disk-rotating motor. As a safety feature, the program also monitors the compressor temperature and refrigerant pressure. If conditions stray beyond preprogrammed limits, an emergency shutdown is performed.

3.4 Performance Calculation

The air-side capacity was calculated using the air flow rate and the air enthalpy difference between inlet and outlet of the evaporator. The refrigerant-side capacity was calculated using the enthalpy difference of the refrigerant across the evaporator and the mass flow rate of the refrigerant. The enthalpies of the refrigerant were calculated by REFPROP V4.01 [6] from the temperature and pressure measurements. ASHRAE Standard 116-1983 requires that the capacities determined using these two methods should agree within 6% of each other. The deviation between the air-side and refrigerant-side values were within 3% for the whole tests presented in this report. Hereafter only the air-side values are presented. The refrigerant-side values were used to check the validity of the measurement.

3.5 Test Procedures

Prior to beginning data acquisition for any test, the entire system was brought to steady-state at the desired test conditions. This was done by first setting the controllers of the indoor loop and outdoor chamber to the appropriate temperature and relative humidity, then running the heat pump

system continuously until all system conditions had been stable for about ½ hour. This included all refrigerant loop temperatures and pressures as well as air temperatures and the condenser's water bath temperature. Beginning a test from this steady state ensured that the thermal mass of system components did not affect the test results. This process usually took about an hour, depending on the test conditions desired. Once conditions were right, the actual test could begin. For steady-state tests this meant simply entering a filename, test length, and desired data-sampling interval into the data-acquisition program, and initiating a data-collection session while the heat pump system continued to run. For cyclic tests the procedure was essentially the same, except that beginning the test initiated the preprogrammed on/off cycle.

4.0 TEST RESULTS AND DISCUSSION

4.1 Charge Optimization Test Results at ASHRAE Test A

System charge optimization was carried out using TEST A of ASHRAE Standard 116-1983. [3] It should be noted that first, the charge optimization tests were conducted at the ASHRAE A test conditions because it was very hard to achieve ASHRAE B test conditions. The humidity control of the chamber was very much affected by the outdoor humidity because the fresh outdoor air was supplied into the chamber to control the humidity. Therefore most tests were conducted when the outdoor humidity was low at night. Cooling capacity and COP were measured for various charges of R-22 at different short tube restrictor sizes. The optimum charge was found at the charge which corresponded to the highest COP and capacity.

The results of the charge optimizations are shown in Figure 4. The plot shows that the COP increases up to a maximum and then decreases, as the charge increases for each ST. In each ST, the point of maximum COP is taken as the optimum charge. If there are two points of maximum COP, the point with maximum COP and capacity is taken as the optimum charge. Note that in Figure 4, ST=0.071", one cannot assume an optimum charge because the COP curve has no absolute maximum. This is because at 9.0 lb of charge, the refrigerant was two-phase at the ST inlet, indicating insufficient subcooling. Therefore, it was necessary to increase charge to increase subcooling.

The optimum charge of each ST was chosen as shown in Table 2. As the diameter of STs increases, the refrigerant mass flow rate increases. Then the optimum charge decreases accordingly. The increased mass flow rate causes a better heat transfer in the heat exchanger and makes the pressure ratio be reduced. The larger ST has a benefit of the lower discharge temperature due to the reduced superheat and condensing pressure. While the excessively large ST reduces the superheat too much, two phase flow might be supplied to the compressor. Therefore, the balancing of these two factors is required. While keeping this point in mind, the best combination of charge and ST was chosen as 10.0 lb charge and 0.067" ST. The test results are shown in Table 2.

Table 2 Optimum Charge Test Results for Each ST at ASHRAE Test A Condition

	Air cooled Condenser	Evaporative Condenser		
Short Tube [inch]	0.065	0.065	0.067	0.069
Refrigerant Charge [lb]	8.0	10.0	10.0	9.5
Capacity [kW]	6.82	7.53	7.49	7.42
COP	3.20	3.23	3.44	3.42
Tdischarge [°C]	76.3	82.7	73.5	71.4
Tsuction [°C]	18.0	25.2	18.7	17.7
Pcond [kPa]	1641.8	1563.4	1380.7	1349.7
Pevap [kPa]	707.5	677.7	641.9	659.4
Pressure Ratio	2.32	2.31	2.15	2.05
Ref. Mass flow rate [kg/s]	0.0446	0.0441	0.0456	0.0465

Table 3 Steady State ASHRAE Test Results

Test Condition	ASHRAE A		ASHRAE B		ASHRAE C	
	R-22 Baseline	Evaporative Condenser	R-22 Baseline	Evaporative Condenser	R-22 Baseline	Evaporative Condenser
Short Tube [inch]	0.065	0.067	0.065	0.067	0.065	0.067
Refrigerant Charge [lb]	8.0	10.0	8.0	10.0	8.0	10.0
Capacity [kW]	6.82	7.49	7.34	7.64	6.62	6.76
COP	3.20	3.44	3.78	3.65	3.48	3.20
Tdischarge [°C]	76.3	73.5	74.3	73.6	67.1	59.2
Tsuction [°C]	18.0	18.7	22.5	22.8	13.2	15.4
Pcond [kPa]	1641.8	1380.7	1379.7	1285.1	1350.5	1178.3
Pevap [kPa]	707.5	641.9	670.0	637.9	631.2	558.8
Pressure Ratio	2.32	2.15	2.06	2.01	2.14	2.11
Ref. mass flow rate [kg/s]	0.0446	0.0456	0.0428	0.0443	0.0410	0.0395

4.2 System Performance Test Results with Charge Optimized at ASHRAE Test A

After conducting the soft optimizations, ASHRAE Tests A, B, C, and D were run at the determined optimum charge and short tube restrictor size. The results of steady state tests are shown in Table 3. The results of cyclic tests are compared with other cases in Table 4.

As can be seen from the Table 3, the ASHRAE A Test has the most benefit of improving the capacity by 9.8% and the COP by 7.5% as compared to the baseline which uses the air cooled condenser. The cooling capacities of the ASHRAE Tests B and C were improved by 4.1% and 2.1%, but the COPs of the ASHRAE Tests B and C were degraded by 3.4% and 8.0% respectively.

The cyclic performance of the evaporative condenser was degraded by 28.8% as compared to the baseline.

Table 4 Cyclic ASHRAE Test Results

Test Condition	ASHRAE D	
	R-22 Baseline	Evaporative Condenser
System		
Short Tube [inch]	0.065	0.067
Charge [lb]	8.0	10.0
CLF	0.182	0.178
C_D	0.198	0.255

The evaporative condenser had reduced operating pressures, while maintaining the similar subcooling and increased superheat. This means that this system has a better heat release in the condenser. This results in lower operating pressures and better performance. But this benefit was most pronounced in ASHRAE Test A and did not manifest itself in the others. Therefore, more careful optimization is required to improve overall performance.

4.3 Charge Optimization Test Results at ASHRAE Test B

To improve the overall performance of the evaporative condenser, especially at the lower humidity condition, it was required to improve the humidity control of the chamber first. It was hard to control the humidity in the chamber because the air-handling unit of the chamber has the smaller dehumidification capacity than the humidification capacity of the evaporative condenser. Therefore, the outdoor unit was modified such that the humid outlet air from the evaporative condenser can be exhausted to the outside directly. After this modification, it was much easier than before to attain the ASHRAE Test Conditions.

The second charge optimization was performed at ASHRAE Test B condition. This optimization was done to balance the benefit of an evaporative condenser throughout all cooling tests and finally to improve the seasonal performance. The ST was chosen as 0.067" which was selected from the charge optimization at ASHRAE Test A condition. As shown in Table 5, the optimum charge was decided as 9.0 lb which is 1.0 lb less than the optimum charge at ASHRAE Test A.

Figure 4 Charge Optimization with Various Short Tube Sizes
ASHRAE Test A, R-22

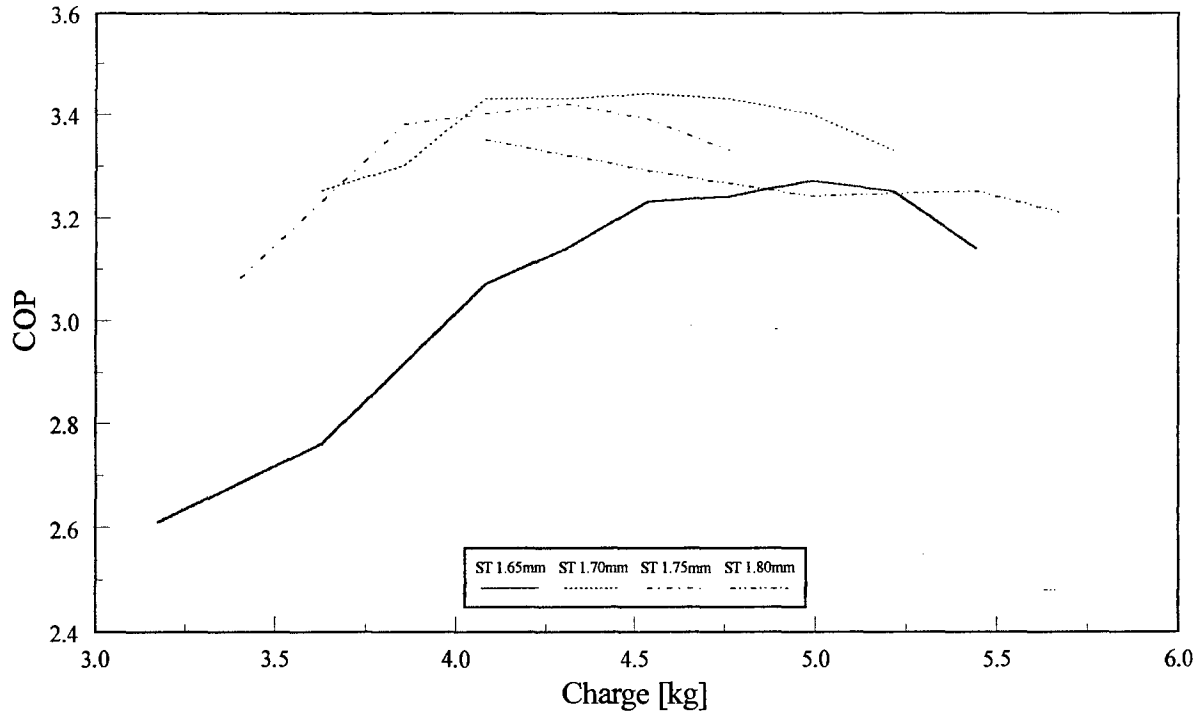
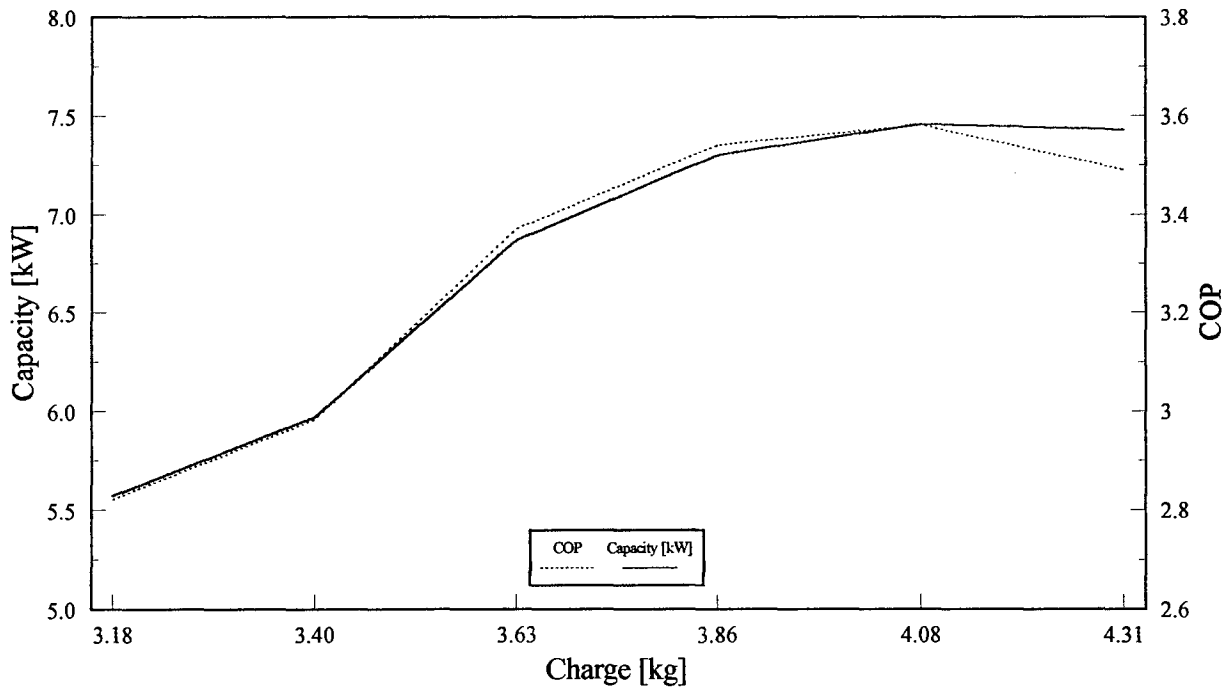


Figure 5 Charge Optimization at ASHRAE Test B



Short Tube: 1.70 mm

Table 5 Optimum Charge Test Results at ASHRAE Test B Condition (ST: 0.067")

Refrigerant Charge [lb]	7.0	7.5	8.0	8.5	9.0	9.5
Capacity [kW]	5.57	5.97	6.87	7.30	7.46	7.43
COP	2.82	2.98	3.37	3.54	3.58	3.49
Tdischarge [°C]	88.9	86.8	80.8	77.8	76.6	72.8
Tsuction [°C]	29.8	29.4	27.5	26.0	25.0	17.6
Pcond [kPa]	1164.6	1182.9	1221.2	1245.7	1259.6	1429.7
Pevap [kPa]	653.8	686.8	770.9	799.8	807.6	885.9
Pressure Ratio	1.78	1.72	1.58	1.56	1.56	1.61
Ref. Mass flow rate [kg/s]	0.0329	0.0326	0.0386	0.0408	0.0419	0.0454

4.4 Airflow Optimization Test Results at ASHRAE Test B

The original duct in the evaporative condenser had an imbalanced airflow distribution. Especially, it has a higher speed in the left half. To improve the airflow distribution across the duct, two different remedies were tested. The first one was adding honeycomb type baffles inside the duct. The second one was installing finer baffles only in the left half. The results are shown in Table 6. The air flow rate decreases and reduces the fan power due to the decreased airflow rate. But this benefit does not turn into an improvement of the performance because the condensing temperature increases as a result. When the baffles were used in the full area across the duct, the performance was almost the same as in the case of no baffles, while the performance decreased a little bit when the finer baffles were used in the left half area. Therefore, it was decided to use the baffles in the full area for the later tests.

4.5 Wheel Disk Speed Optimization Test Results at ASHRAE Test B

To find out the wheel speed for optimum COP experimentally, the wheel speed was varied as shown in Table 7. As the wheel speed increases, the condensing temperature decreases due to the better mass transfer. But at the same time, more motor power is required which is a disadvantage. Therefore an optimum wheel speed exists and it was found at 30 rpm. This speed was set for the later tests.

Table 6 Airflow Optimization Test Results (Charge: 9.0 lb, ST: 0.067")

Airflow Condition	No Baffles	Baffles in Full Area	Baffles only Left Half Area
Capacity [kW]	7.46	7.42	7.33
COP	3.58	3.58	3.55
Tdischarge [°C]	76.6	76.1	78.0
Tsuction [°C]	25.0	24.5	24.0
Tcondensing [°C]	32.2	32.3	34.7
Pcond [kPa]	1259.6	1263.6	1345.3
Pevap [kPa]	620.7	625.6	635.0
Pressure Ratio	2.03	2.02	2.12
Fan and Wheel Motor Power [kW]	0.394	0.373	0.294
Ref. Mass flow rate [kg/s]	0.0419	0.0421	0.0427

Table 7 Wheel Rotation Speed Optimization Test Results (Charge: 9.0 lb, ST: 0.067")

Wheel Rotation Speed [rpm]	15	30	45
Capacity [kW]	7.56	7.47	7.43
COP	3.60	3.63	3.57
Tdischarge [°C]	75.4	76.9	76.8
Tsuction [°C]	22.8	24.8	25.9
Tcondensing [°C]	33.6	32.4	30.6
Pcond [kPa]	1305.4	1268.5	1210.9
Pevap [kPa]	637.6	622.7	604.0
Pressure Ratio	2.05	2.04	2.00
Fan and Wheel Motor Power [kW]	0.361	0.365	0.439
Ref. Mass flow rate [kg/s]	0.0432	0.0418	0.0406

4.6 Steady State Performance Test Results

The second set of ASHRAE Tests A, B, C, and D were run at the determined optimum charge, baffles, and wheel rotation speed. The steady state test results are shown in Table 8. The cyclic test results are compared with other cases in Table 9. As shown in Table 8, the ASHRAE Test A has the most benefit of improving the capacity by 8.1% and the COP by 5.6% as compared to the

base line which uses the air cooled condenser. The cooling capacities of the ASHRAE B and C Tests were improved by 1.8% and 5.7% respectively, but the COPs of the ASHRAE B and C Tests were degraded by 4.0% and 2.0% respectively. In overall, the performance improvement at ASHRAE A was reduced, while the performance at ASHRAE B and C was improved as compared to those tests optimized at ASHRAE Test A. This means a better balance through all tests, meaning a better seasonal performance.

Table 8 Steady State ASHRAE Test Results

Test Condition	ASHRAE A		ASHRAE B		ASHRAE C	
	R-22 Baseline	Evaporative Condenser	R-22 Baseline	Evaporative Condenser	R-22 Baseline	Evaporative Condenser
Short Tube [inch]	0.065	0.067	0.065	0.067	0.065	0.067
Refrigerant Charge [lb]	8.0	9.0	8.0	9.0	8.0	9.0
Capacity [kW]	6.82	7.37	7.34	7.47	6.62	7.00
COP	3.20	3.38	3.78	3.63	3.48	3.41
Tdischarge [°C]	76.3	78.7	74.3	76.9	67.1	70.0
Tsuction [°C]	18.0	23.7	22.5	24.8	13.2	16.8
Pcond [kPa]	1641.8	1363.4	1379.7	1268.5	1350.5	1200.8
Pevap [kPa]	707.5	643.5	670.0	622.8	631.2	589.6
Pressure Ratio	2.32	2.12	2.06	2.04	2.14	2.04
Ref. mass flow rate [kg/s]	0.0446	0.0434	0.0428	0.0418	0.0410	0.0404

It should be noted that by proper adjustments in the design, COP improvements can be traded in for capacity improvements and vice versa.

4.7 Cyclic Performance Test Results

The cyclic performance of the evaporative condenser was improved by 18.7% as compared to the baseline in terms of C_D . The better balance of the steady state performance and the improvement of cyclic performance improved the seasonal performance as close to that of the baseline as shown in Table 9. The seasonal performance was calculated based on the U.S.A. national average climate weighted in proportion to air-conditioner sales data as published by ASHARE. The seasonal performance of ASHRAE A optimization was 6.0 % lower than that of the baseline, while the seasonal performance of ASHRAE B optimization was just 1.7 % lower than that of the baseline.

Table 9 Seasonal Performance Test Results

System	R-22 Baseline	Evaporative Condenser	
	at ASHRAE Test B	at ASHRAE Test A	at ASHRAE Test B
Charge Optimization			
Short Tube [inch]	0.065	0.067	0.067
Refrigerant Charge [lb]	8.0	10.0	9.0
CLF	0.182	0.178 (- 2.2 %)	0.183 (+ 0.1 %)
C _D	0.198	0.255 (+ 28.8 %)	0.161 (- 18.7 %)
SEER	11.7	11.0 (- 6.0 %)	11.5 (- 1.7 %)

4.8 Fan and Wheel Motor Power Compensation Results

The power of the outdoor fan motor is greater than what is needed in an actual system because the fan motor was oversized to overcome the additional flow resistance by the duct used to maintain the required test conditions for the air. The wheel motor consumes more energy because an inverter driven motor was used in the test to easily control the wheel speed; in an actual installation, a single-speed motor would be acceptable. Therefore, it is reasonable to compensate for the parasite power for a fair comparison. Table 10 shows the differences. In this table, the fan and wheel motor power were estimated based on static pressure difference across the wheel, air flow rate, and torque requirement. Based on these, the fan and wheel motor powers were estimated as 49.2 and 32.9 W respectively. [2] The compensation was performed such that the difference between the lowest power consumption at ASHRAE Test B and this power estimation is subtracted from all test results.

Table 10 Fan and Wheel Motor Power Compensation

Test Condition	ASHRAE A	ASHRAE B	ASHRAE C
Indoor Fan Power [kW]	0.268	0.263	0.275
Compressor Power [kW]	1.516	1.435	1.374
Measured Outdoor Fan/Wheel Power [kW]	0.395	0.365	0.408
Estimated Outdoor Fan/Wheel Power [kW]	0.112	0.082	0.125
Power before Compensation [kW]	2.179	2.063	2.057
Power after Compensation [kW]	1.896	1.780	1.774

With these compensated power values, the COPs were recalculated and compared as shown in Tables 11 and 12. As can be seen in Table 11, the steady state COPs were improved very much and 11.1 to 21.6 % higher than that of the baseline. The improvement in cyclic performance shown by the evaporative condenser was not as great after adjustment (although still improved) because all

COPs were improved. The better COPs of the steady state performance and the improvement of cyclic performance improved the seasonal performance by 14.5% above the baseline as shown in Table 12.

Table 11 Compensated Steady State ASHRAE Test Results

Test Condition	ASHRAE A		ASHRAE B		ASHRAE C	
	R-22 Baseline	Evaporative Condenser	R-22 Baseline	Evaporative Condenser	R-22 Baseline	Evaporative Condenser
Capacity [kW]	6.82	7.37 (+ 8.1 %)	7.34	7.47 (+ 1.8 %)	6.62	7.00 (+ 5.7 %)
COP before Compensation	3.20	3.38 (+ 5.6 %)	3.78	3.63 (- 4.0 %)	3.48	3.41 (- 2.0 %)
COP after Compensation	n/a	3.89 (+ 21.6 %)	n/a	4.20 (+ 11.1 %)	n/a	3.95 (+ 13.5 %)

Table 12 Compensated Seasonal Performance Test Results

System	R-22 Baseline	Evaporative Condenser	
Compensation	n/a	before correction	after correction
CLF	0.182	0.183 (+ 0.1 %)	0.183 (+ 0.1 %)
C_D	0.198	0.161 (- 18.7 %)	0.144 (- 27.3 %)
SEER	11.7	11.5 (- 1.7 %)	13.4 (+ 14.5 %)

4.9 Thermal Storage Effect Test Results

To examine the possibility of further improvement of the cyclic performance, a modified cyclic performance test was performed. In this test, the outdoor fan and wheel motor were operated continuously during the compressor off period. Therefore only the compressor was turned on for 6 minutes and off for next 24 minutes, while the other components were kept running. In this test, the water bath temperature drops due to the continuous mass and heat transfer between the water film on the wheels and the airflow. By this heat removal during the compressor off period, it is possible to reduce the condensing temperature during the compressor on period. Thus we use the cold thermal storage effect during the on period by exhausting heat during the off period.

Figures 6 and 7 show two-different cases; the first one is the normal cyclic operation and the second one is the modified cyclic operation. As can be seen in these figures, the water bath temperature of the first one changes only approximately 1 C°, but that of the second one changes approximately 3 C°. The latter one has the benefit of the lower condensing temperature due to the thermal storage effect during the off period. On the other hand, the latter one has the disadvantage of consuming more energy by operating the outdoor fan and wheel motor during the off period. This disadvantage becomes a penalty; the cyclic degradation coefficient C_D increased to 0.505. Another possibility is just operating the outdoor fan and wheel motor for a few minutes during the immediate

Figure 6 Cyclic Test (ASHRAE Test D)
Compressor, Outdoor Fan & Wheel All Cycle

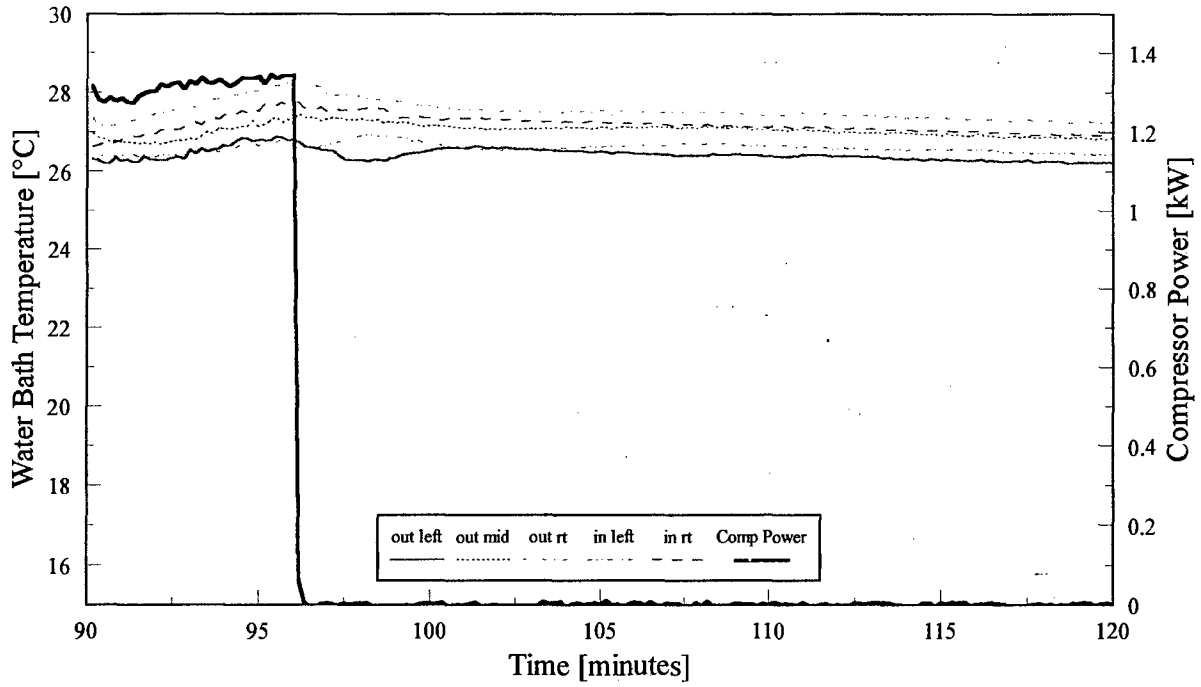
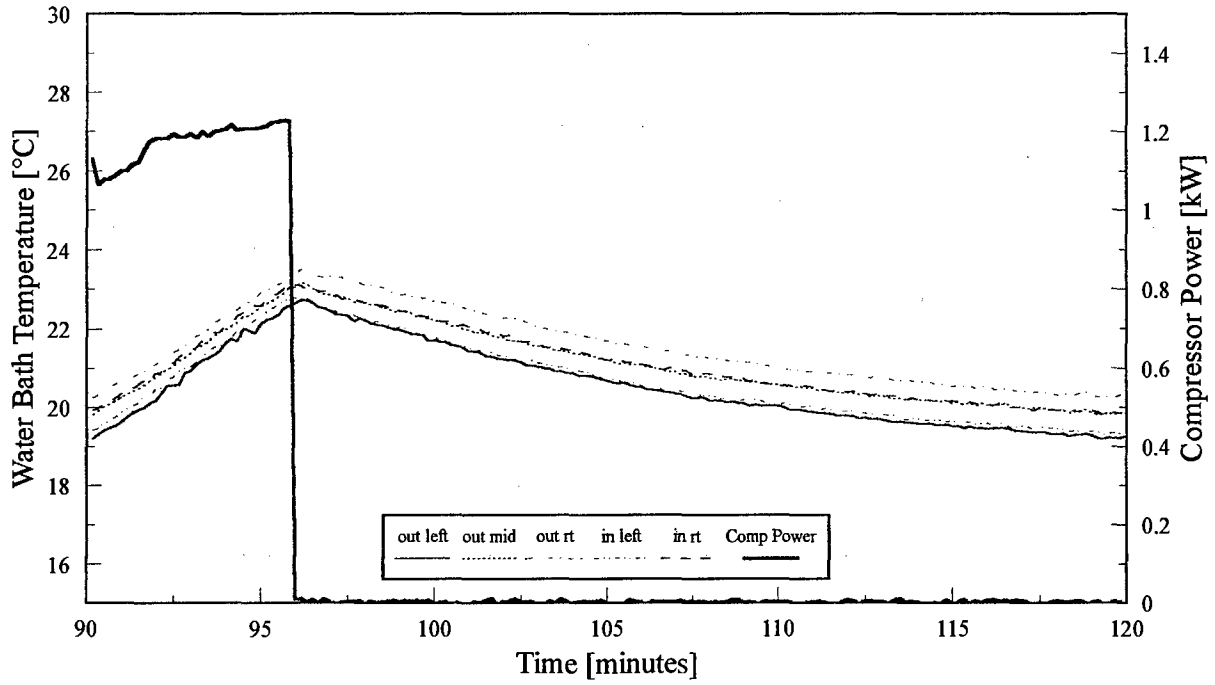


Figure 7 Cyclic Test (ASHRAE Test D)
Outdoor Fan & Wheel Running Continuously



off period to minimize the additional power for the thermal storage. To be able to have a thermal storage benefit, the water temperature should drop more than 1 C° of the normal cycle during this short period. Unfortunately, the water bath temperature drops slowly as shown in Figure 7. This means that the utilization of the thermal storage effect is not an effective way to improve cyclic performance.

5.0 CONCLUSIONS

A novel full-scale evaporative condenser was experimentally evaluated. Soft optimization was performed to maximize the benefit of the evaporative condenser. The soft optimization was carried out to choose the best combination of the ST size and refrigerant charge. The design parameters of the evaporative condenser, airflow and wheel rotation speed were optimized.

The final system specification shows improved steady performance and compatible seasonal performance with the baseline; cooling capacity ranging from 101.8 to 108.1 %, COP ranging from 98.0 to 105.6 %, and SEER of 98.3 %. After accounting for the excessive power consumption by the outdoor fan motor and wheel motor (excess power beyond that needed for normal operation to accommodate additional testing requirements), the evaporative condenser showed significant improvement. The evaporative condenser has a higher capacity by 1.8 to 8.1 %, a higher COP by 13.5 to 21.6 %, and a higher SEER by 14.5 % than those of the baseline.

The condensing temperature of the evaporative condenser is limited by the wet bulb temperature of the air. Therefore the evaporative condenser has the advantage of a lower condensing temperature than that of an air-cooled condenser. The lower condensing temperature reduces the work done by the compressor. The lower compressor power and the lower outdoor fan and wheel motor power increase the COP and SEER.

ACKNOWLEDGMENT

The support for this work by the U.S. Environmental Protection Agency, the Engineering Research Center, and the CEEE at the University of Maryland is gratefully acknowledged.

REFERENCES

- [1] American Society of Heating, Refrigerating and Air-Conditioning Engineers, Inc., 1988, "1988 ASHRAE Handbook: Equipment"
- [2] Markey, Brian A., 1996, "The Evaporatively Cooled Condenser," Master's Thesis submitted to University of Maryland, Graduate School.
- [3] American Society of Heating, Refrigerating and Air-Conditioning Engineers, Inc., 1983, "Methods of Testing for Seasonal Efficiency of Unitary Air-Conditioners and Heat Pumps," ASHRAE Standard ANSI/ASHRAE 116-1983.

- [4] Air-Conditioning and Refrigeration Institute, 1989, "Unitary Air-Conditioning and Air Source Heat Pump Equipment," ARI Standard 210/240-1989.
- [5] American National Standards Institute, 1985, "Laboratory Methods of Testing Fans for Rating," ANSI Standard 210-1985.
- [6] Gallagher J., McLinden M., and Huber M., 1993, "REFPROP" NIST Thermodynamic Properties of Refrigerants and Refrigerant Mixtures Database, Version 4.01, Thermophysics Division of National Institute of Standards and Technology, Gaithersburg, MD.

Appendix A

A-1 Evaporative Condenser Performance Evaluation

The performance of an evaporative condenser can be divided into a steady state performance and a seasonal performance. Test methods for measuring performance were based on the ASHRAE Standard 37-1988 "Methods of Testing for Rating Unitary Air-conditioning and Heat Pump Equipment", ASHRAE Standard 116-1983 "Methods of Testing for Seasonal Efficiency of Unitary Air-conditioners and Heat Pumps", and ARI Standard 210/240-1989 "Unitary Air-conditioning and Air-source Heat Pump Equipment".

A-1.1 Steady State Performance

The steady state performance of an evaporative condenser is evaluated by determining the capacity and coefficient of performance (COP). COP is the ratio of the rate of heat delivered to the conditioned space to the rate of energy input. Cooling test conditions A, B, and C are test conditions for steady state operation.

During steady state tests, the capacity is calculated using the following equations, based on the air enthalpy method and the refrigerant enthalpy method. In the air enthalpy method, the total capacity is calculated as a sum of sensible and latent capacity. The sensible capacity (q_{si}) is calculated from the air flow rate (Q_{mi}), the air temperature entering the indoor unit (T_{ain}), and the air temperature exiting the indoor unit (T_{aout}). The air flow rate (Q_{mi}) for the indoor unit through a single nozzle is calculated by the following equations with the static pressure difference across nozzle (p_v), the absolute pressure (p_n), the temperature (T_n), and the humidity ratio at the nozzle throat (W_n).

$$Q_{mi} = 1.414 C A_n Y (1000 p_v v_n^*)^{0.5} \quad [m^3/s] \quad (1)$$

- where C: Coefficient of discharge for a nozzle, $C = 0.99$
A_n: Nozzle area [m²]
Y: Expansion factor for a nozzle given in ASHRAE 51-1985.
p_v: Static pressure difference across a nozzle [Pa]
v_n*: Specific volume of air at nozzle calculated by equation (2).

$$v_n^* = 101 \frac{v_n}{p_n (1+W_n)} \quad [m^3/kg] \quad (2)$$

- where p_n: Pressure at a nozzle [kPa]
v_n: Specific volume of air at a nozzle but at standard barometric pressure calculated by perfect gas equation (3).

$$v_n = \frac{0.287 (T_n + 273.15)}{101.325} (1 + 1.6078W_n) \quad [m^3/kg] \quad (3)$$

where T_n : Temperature at nozzle throat [$^{\circ}C$]
 W_n : Humidity ratio at nozzle throat calculated by equation (4).

$$W_n = 0.622 \frac{p_{ws}}{(p_n - p_{ws})} \quad (4)$$

where p_{ws} : Saturated pressure of water calculated by the correlation in ASHRAE Fundamental-1993 [1] with the temperature at nozzle (T_n) [kPa]

Then the sensible capacity (q_{si}) is calculated by equation (5).

$$q_{si} = \frac{Q_{mi}}{v_n^* (1 + W_n)} c_{pa} (T_{ain} - T_{aout}) \quad [W] \quad (5)$$

The latent capacity (q_{lci}) is calculated from the humidity ratio difference between inlet and outlet by equation (6).

$$q_{lci} = 2.47 \times 10^6 \frac{Q_{mi}}{v_n^* (1 + W_n)} (W_{iin} - W_{iout}) \quad [W] \quad (6)$$

where W_{iin} : Humidity ratio entering the indoor unit
 W_{iout} : Humidity ratio leaving the indoor unit

The refrigerant enthalpy method is another way to obtain the capacity. The refrigerant mass flow rate and the refrigerant enthalpies at the inlet and outlet of a heat exchanger should be obtained to calculate the refrigerant side capacity. The mass flow rate (m) of the refrigerant can be measured directly by a mass flow meter, and the refrigerant enthalpies are calculated by the REFPROP database V4.0 from temperature and pressure measurements of the refrigerant in the single phase region. Then the capacity is calculated from the energy balance for the indoor coil by an equation (7) for cooling (q_{lci}).

$$q_{tci} = m (h_{rout} - h_{rin}) - E_i \text{ [W]} \quad (7)$$

where m: Refrigerant mass flow rate [kg/s]
 h_{rin} : Enthalpy of refrigerant entering the indoor unit [J/kg]
 h_{rout} : Enthalpy of refrigerant leaving the indoor unit [J/kg]
 E_i : Power input into indoor fan motor [W]

A-1.2 Cyclic Performance

The cyclic behavior of an evaporative condenser is very important because the unit is actually operating in a cyclic manner to balance the capacity and the load. Cyclic tests for cooling and are used to measure the transient performance. In cyclic tests, the capacity and COP of the transient case can be as compared to those of the steady state case by the following three terms.

(1) Cooling Load Factor (CLF), Cooling

CLF is a ratio of the total cooling capacity of a complete cycle for a specified period consisting of an "on" time and "off" time to the steady-state cooling capacity over the same period at constant ambient conditions.

$$CLF = \frac{Q_{cyc,dry}}{Q_{ss,dry}} \quad (8)$$

where $Q_{cyc,dry}$: Cyclic capacity during one "on" and "off" cycle measured at ASHRAE cyclic cooling test (D).
 $Q_{ss,dry}$: Steady state capacity for the same duration measured at ASHRAE cooling test C.

(2) Degradation Coefficient (C_D)

C_D is a factor of efficiency loss due to the cycling of the unit. The C means a degradation coefficient that is the factor of efficiency loss due to the cycling of the unit.

$$C_D = \frac{1 - \frac{COP_{cyc,dry}}{COP_{ss,dry}}}{(1 - CLF)} \quad (9)$$

So C_D can be interpreted as the ratio of COP decrease as compared to the capacity decrease.

A-1.3 Seasonal Performance

To simulate the real performance of an evaporative condenser during the cooling season, the seasonal efficiency for cooling are defined based on the steady state and cyclic performance. These efficiencies are evaluated by a BIN method that is a hand calculation procedure where energy requirements are determined at many outdoor temperature conditions. The temperature bins are usually 5 °F (2.8 °C) in size.

(1) Seasonal Energy Efficiency Ratio (SEER), Cooling

SEER is a ratio of the total heat removed, in Btu, during the normal usage period for cooling to the total energy input, in watt-hours, during the same period. SEER can be calculated from following equations [2].

$$SEER = \sum q(t_j) / \sum E(t_j) \quad [Btu/kWhr] \quad (10)$$

where $q(t_j)$: Cooling capacity at each Bin temperature (t_j), $q(t_j) = (CLF) q_{ss}(t_j) n_j$
 $E(t_j)$: Power input at each Bin temperature (t_j), $E(t_j) = (CLF) E_{ss}(t_j) n_j / PLF$

where $CLF = BL(t_j) / q_{ss}(t_j)$ for $BL(t_j) \leq q_{ss}(t_j)$ or $CLF = 1$ for $BL(t_j) > q_{ss}(t_j)$
 PLF: Part Load Factor, $PLF = 1 - C_D [1 - (CLF)]$

The building load $BL(t_j)$ is calculated from equation (11).

$$BL(t_j) = \frac{(5j - 3)}{(t_{OD} - 65)} \frac{q_{ss}(t_{OD})}{SizeFactor} \quad (11)$$

where j : Temperature Bin
 t_j : Representative temperature of the j th bin, $t_j = 62 + 5j$ [°F]
 t_{OD} : Outdoor Design Temperature
 Size factor: Amount of oversizing desired, Size factor = 1.1

A-2 Instruments

Instruments were installed to obtain all data satisfying ASHRAE Standard 116 [2].

A-2.1 Temperature Measurement

T type, copper-constantan, thermocouples were used in measuring the air stream and the refrigerant temperatures. The thermocouples were calibrated at the freezing and boiling point of water. At the freezing point, the average temperature deviation was within ± 0.1 °C and it was within ± 0.25 °C at the boiling point.

To measure the inlet and outlet air stream temperature of an indoor unit, two of the nine grid thermocouples were located after the air mixer at the inlet and outlet of the test unit. For the outdoor unit, nine thermocouples were installed at the inlet, while the outlet temperatures were measured by five thermocouples after the extended duct to prevent the recirculation of the air stream. The refrigerant temperatures were measured by soldering thermocouples on the top and bottom of the refrigerant pipes. The refrigerant temperatures for the top and bottom were averaged to obtain a proper temperature reading.

The humidity ratio is essential to determine the capacity of the test unit. The humidity ratio was measured by a General Eastern m2/111h/t-100 dewpoint meter, having NIST traceable accuracy of ± 0.20 °C (0.36 °F) at 26.7 °C (80 °F) and 40% RH.

A-2.2 Pressure Measurement

Atmospheric pressure was measured by the mercury column style barometer. The static pressures for the indoor loop were measured with the differential pressure transducers having an accuracy of ± 0.4 % of the reading. They had a range of 0 to 12.7 cm (5") water column. Absolute pressure transducers with a range of 0 to 3447 kPa (500 psi) were used in measuring the refrigerant pressures, having an accuracy of $\pm 0.11\%$ of the full scale reading. The compressor discharge, downstream of the flow meter, indoor unit inlet and outlet, and suction pressure were measured with this transducer.

A-2.3 Air Flow Rate Measurement

The air flow rate was measured by a nozzle apparatus. The nozzle diameter was selected to maintain the throat velocity within the recommended velocity range of 15.2 - 35.6 m/s. The diameter of the nozzle was measured with a precision micrometer. The micrometer had an accuracy within 5.1×10^{-3} cm (2×10^{-3} in). The static pressure drops across the nozzle and the indoor unit were measured with differential pressure transducers having an accuracy of ± 0.4 % of the full scale reading.

The air flow rate (Q_{mi}) for the indoor unit through a single nozzle is calculated from equations (1), (2), (3), and (4) with measured parameters; the static pressure difference, and the humidity ratio (W_n) at the nozzle throat.

The air flow rate was calibrated with a electric heater installed at the bottom of the indoor unit. The power to the heater and the fan motor (q_{heatin}) were measured. The inlet and outlet enthalpies of the indoor coil were measured via the average air stream temperatures (T_{ain} , T_{aout}) and the inlet humidity ratio. The air flow rate can be calculated from the energy balance for the indoor unit based on these values by equation (12).

$$Q_{cal} = \frac{q_{heatin}}{(h_{ain} - h_{aout})} v_n^* (1 + W_n) \quad [m^3/s] \quad (12)$$

where q_{heatin} : Heater and fan motor power input [W]
 h_{ain} : Air stream enthalpy at inlet of indoor unit calculated by equation (13) [2]
 h_{aout} : Air stream enthalpy at outlet of indoor unit calculated by equation (13)

$$h = 1006 T + W(2501000 + 1860 T) \quad [J/kg] \quad (13)$$

The deviation of air flow rate between by the air enthalpy method and by the nozzle static pressure difference was 2.9% on average.

A-2.4 Electrical Instruments

The input power and line voltage to the indoor and outdoor unit were separately measured. The watt transducer had an accuracy of ± 0.2 % of the full scale reading and had a full scale reading of 4 kW. The voltage measurement was made with an Ohio Semitronics volt transmitter VT-240a that has an accuracy of ± 0.5 % of the full scale reading.

A-2.5 Refrigerant Mass Flow Measurement

The refrigerant mass flow rate was measured by a Coriolis based mass flow meter, Micro Motion D-25. It has an accuracy of ± 0.4 % of full scale for the mass flow rate. The flow meter was

connected to the liquid line, upstream of the expansion device. To keep the inlet condition as a liquid whether in cooling or heating mode, two bypass lines and four shut-off valves were installed on the vapor line. This inlet condition was checked by a sight glass installed downstream of the meter.

A-2.6 Time and Weight Measurements

The time was maintained by the internal clock of an IBM compatible computer having an accuracy of $\pm 0.05\%$. The Electronic scale having an accuracy of 1×10^{-4} kg (2.2×10^{-4} lb) was used for charging the refrigerant or the oil into the system as well as on weighing the condensate.

A-3 Uncertainty Analysis

The performance of a test unit is characterized by the parameters such as the cooling capacities, the steady state and cyclic coefficient of performance (COP), the cooling load factor (CLF), and the cooling degradation coefficient (C_D). When calculating these values, all measured data were used with the equations described in ASHRAE Standard 116-1983 and ARI Standard 210/240-1989.

The total experimental uncertainty in the measurement and calculation is classified by bias error (systematic error) and random error (precision error). The bias error is determined using the Pythagorean summation of the discrete uncertainties as shown in the following equation.

$$u_f = \sqrt{\left(u_{x1} \frac{\partial f}{\partial X_1}\right)^2 + \left(u_{x2} \frac{\partial f}{\partial X_2}\right)^2 + \dots + \left(u_{xn} \frac{\partial f}{\partial X_n}\right)^2} \quad (14)$$

where u_f : The overall uncertainty of function f resulting from the individual uncertainties of $x_1 \dots x_n$.

x_i : Nominal values of variables

u_{xi} : Discrete uncertainties

The individual uncertainties, u_x , are already explained in Section A-2. The results of bias errors which are calculated using equation (14) based on the discrete uncertainties are shown in Table A-1.

Table A-1 Estimated Bias Errors of Characteristic Parameters

Parameters	Capacity	COP	CLF / HLF	C_D
Mode	Steady State	Steady State	Cyclic	Cyclic
Bias Error	$\pm 1.5\%$	$\pm 1.5\%$	$\pm 2.1\%$	$\pm 8.2\%$

[Note] CLF: Cooling Load Factor, HLF: Heating Load Factor, C_D : Cyclic Degradation Coefficient

Table A-1 shows very large bias error for C_D due to the form of the equation which defines C_D .

The random error is analyzed using statistical methodology. The Gaussian probability distribution is assumed for the test data because the data being studied are derived from experiment. The standard deviation, σ , is calculated using equation (15).

$$\sigma = \sqrt{\frac{\sum x_i^2 - n x_m^2}{n - 1}} \quad (15)$$

where σ : Standard deviation
 n: number of data
 x_i : The magnitude of the measured quantity
 x_m : The arithmetic mean value

Three-sigma error ($\pm 3\sigma$) which has 99.7% certainty if the data has normal distribution is used as a random error. Twelve sets of data are used in calculating the random errors of steady state parameters and three sets of data are used in calculating the random errors of cyclic parameters. The random errors obtained are shown in Table A-2.

Table A-2 Estimated Random Errors of Characteristic Parameters

Parameters	Capacity	COP	CLF	C_D
Mode	Steady State	Steady State	Cyclic	Cyclic
Random Error	$\pm 1.2\%$	$\pm 1.5\%$	$\pm 1.3\%$	$\pm 2.7\%$

[Note] CLF: Cooling Load Factor, C_D : Cyclic Degradation Coefficient

After evaluating the bias and random errors, the total errors were calculated as shown in Table A-3.

Table A-3 Estimated Total Uncertainty of Characteristic Parameters

Parameters	Capacity	COP	CLF	C_D
Mode	Steady State	Steady State	Cyclic	Cyclic
Total Uncertainty	$\pm 2.7\%$	$\pm 3.0\%$	$\pm 3.4\%$	$\pm 10.9\%$

[Note] CLF: Cooling Load Factor, C_D : Cyclic Degradation Coefficient

A-4 Quality Assurance

A-4.1 Project Responsibility and Personnel

Principal Investigator: Reinhard Radermacher, PhD
Research Assistant: Yunho Hwang
Quality Assurance Supervisor: Keith E. Herold, PhD

The responsibility for quality assurance and for data quality control is shared by all members working on the project. The ultimate responsibility is carried by the principal investigator. In addition, an independent person at the University of Maryland (K. Herold, PhD) functioned as a quality assurance supervisor by regularly checking the recorded and outgoing data.

A-4.2 Experiment Description

A-4.2.1 Test Facility

The test facility was designed to meet or exceed the specifications in ASHRAE Standard 116-1983. During shakedown and actual testing, a series of design improvements were made to the facility to improve functionality through improved control and improved measurement accuracy. These facility details were described in Chapter 2 (pg. 2 of basic report). The project team was guided by a continuous quality improvement philosophy which included frequent discussions of how the various design features were performing and how to make them perform better. This on-going discussion was stimulated by the Quality Assurance supervisor so as to become a basic operating philosophy of the project.

A-4.2.2 Test Arrangements

All tests were performed according to ASHRAE Standard 116-1983 with the loop air-enthalpy method and the refrigerant enthalpy method as a check on accuracy. The arrangement for using the loop air-enthalpy method is illustrated in Figure 1 (pg. 4 of basic report). Care was taken to obtain the highest possible data accuracy. This included a series of quality control including periodic review of the data by the Quality Assurance supervisor and frequent data reviews by the project personnel. These reviews often led to improvements in procedures and in the installation and maintenance of the measuring devices.

A-4.3 Capacity Test Methods

A-4.3.1 Air-Enthalpy Method

The air enthalpy method was the primary data reduction procedure. This method involved performing an energy balance on the air side of the coils to determine capacity. The difficulties involved in this method include: 1) avoiding stratification in the air flow prior to measuring the properties, 2) accurate air flow rate measurement, 3) accurate dry bulb temperature measurement, and 4) accurate humidity measurement. All of these difficulties are addressed in the ASHRAE Standard test procedure. In applying the standard, a series of anomalies were encountered during

shakedown testing. The anomalous results led to additional tests which led ultimately to changes in the facility that solved the individual problems. An example is the wet bulb temperature measurements. The ASHRAE standard specifies a wet bulb measurement system employing a wetted wick. This system was found to be inaccurate and to read consistently off from the more accurate readings subsequently obtained from a high-accuracy dew point sensor system. Once the more accurate system was in place, energy balance results improved considerably. This type of shakedown procedure was employed on all systems until all systems were performing within specifications.

A-4.3.2 Refrigerant Enthalpy Flow Method

In this method, the capacity is determined from the refrigerant enthalpy change and the flow rate. The enthalpy changes were determined from measurements of the entering and leaving evaporator and condenser pressures and temperatures of the refrigerant while the flow rate is determined by a flow meter in the liquid line downstream of the condenser. The refrigerant enthalpy flow method requires detailed property data of the refrigerant applied in the system. The property data is not available from purely experimental data for refrigerants and refrigerant mixtures. The latest version of REFPROP (V4.01) was used to determine the thermodynamic properties of the refrigerant tested and refrigerant mixtures which possibly can be tested. The lack of accurate refrigerant enthalpy data meant that the refrigerant enthalpy method was not used as the primary data reduction method. However, it was found that the results of the two capacity determination methods agreed within $\pm 5\%$ across the board.

A-4.4 Test Procedures

The data taken are summarized in Tables 8-12. The test conditions are summarized in Table 1. The tests performed have been described elsewhere in this report. The quality assurance task stressed the importance of careful procedures to ensure high-quality data. These procedures included extensive shakedown tests. Another key aspect of determining the performance improvement of the evaporative condenser was careful establishment of baseline results.

The shakedown tests were performed initially. The shakedown tests included a complete check on the operational status of all technical equipment. The four reconditioning apparatuses, the two indoor and outdoor test units, and all measuring instrumentation was determined to be operating within expected tolerances.

Baseline tests were performed after the shakedown tests with the original test units and refrigerant R-22. The baseline tests included all tests listed in Table 1 (A, B, C, D)(see page 6). They were used as the basis of comparison of all tests.

A-4.5 Fulfillment of Project Plan

The goal of this project was to provide experimentally derived performance data and to demonstrate the feasibility of the evaporative condenser. These two goals are achieved by carrying out the tests and by examining the feasibility from data. These results are as described in Chapter 4, Test Results and Discussion.

A-5 References

[1] "1993 ASHRAE Handbook: Fundamentals," American Society of Heating, Refrigerating and Air-Conditioning Engineers, Inc., pg. 6.11, 1993.

[2] "Methods of Testing for Seasonal Efficiency of Unitary Air-Conditioners and Heat Pumps," ASHRAE Standard ANSI/ASHRAE 116-1983, American Society of Heating, Refrigerating and Air-Conditioning Engineers, Inc., 1983.